nature photonics

ARTICLES

PUBLISHED ONLINE: 5 MAY 2013 | DOI: 10.1038/NPHOTON.2013.108

Enhanced energy storage in chaotic optical resonators

C. Liu[1], A. Di Falco[2], D. Molinari[1,3], Y. Khan[1], B. S. Ooi[1], T. F. Krauss[2,4] and A. Fratalocchi[1]*

Chaos is a phenomenon that occurs in many aspects of contemporary science. In classical dynamics, chaos is defined as a hypersensitivity to initial conditions. The presence of chaos is often unwanted, as it introduces unpredictability, which makes it difficult to predict or explain experimental results. Conversely, we demonstrate here how chaos can be used to enhance the ability of an optical resonator to store energy. We combine analytic theory with *ab initio* simulations and experiments in photonic-crystal resonators to show that a chaotic resonator can store six times more energy than its classical counterpart of the same volume. We explain the observed increase by considering the equipartition of energy among all degrees of freedom of the chaotic resonator (that is, the cavity modes) and discover a convergence of their lifetimes towards a single value. A compelling illustration of the theory is provided by enhanced absorption in deformed polystyrene microspheres.

The enhanced interaction between light and matter in optical cavity resonators is an interdisciplinary subject of a great interest as it affects many areas of condensed matter physics, including cavity electrodynamics[1], quantum and nonlinear optics, but also more applied aspects such as optical signal processing[2–4] and resonantly enhanced optical absorption[5]. All these applications are enabled by highly optimized optical resonators that can efficiently trap electromagnetic energy in narrow frequency bands. In conventional cavities, there is a simple tradeoff between bandwidth and the enhancement of trapped energy: the higher the enhancement, the narrower the bandwidth. A great challenge in the field is therefore to develop a new generation of cavities that are able to break this fixed relationship and store more energy in a given bandwidth window than conventional cavities would allow. These are expected to provide new breakthroughs in the field, thus accessing a novel series of applications ranging from sensing to lasers, energy harvesting and cavity quantum electrodynamics.

The maximum power that can be transferred into a conventional resonator depends on the coupling coefficient and loss of each given mode, and tends to vary across the mode spectrum, especially when broadband operation ($\Delta\lambda$ on the scale of hundreds of nanometres) is considered. In addition, classical two- and three-dimensional geometries tend to accommodate modes with very different lifetimes in the same spectral region, a good example being the widely used photonic crystal 'L3' type cavity that features modes of very different Q-factor closely spaced in frequency[6]. Therefore, the use of classical resonators for broadband energy storage is limited. Here, we overcome this intrinsic limitation by exploiting specific shape deformations that support chaotic trajectories for light rays. Surprisingly, we note that in a chaotic cavity—regardless of any regime of coupling—the lifetimes of all modes tend towards a common value, thus significantly improving the transfer of energy into the cavity and increasing the energy-storage capability of the cavity. Such chaotic resonators[7] have been well exploited in the field of laser devices[8–15]. We also note that the mode spectrum of deformed microsphere resonators has been studied recently, with remarkable changes in Q-factors being observed[16]. However, despite this large body of literature, nothing is known about the capacity of such resonators to store and collect light energy over a broad spectral range.

The increased energy storage capacity of a chaotic resonator when compared to a classical one can be explained intuitively by adopting a ray optics approach and considering that a suitable shape deformation is accompanied by the breaking of symmetry in the structure. As a consequence, the deformed resonator cannot support any cyclic motion of light, so the trajectory of light rays changes from regular to random, statistically resulting in a larger lifetime of the photons in the cavity[7]. To clarify this result, we start our analysis from a symmetric (classical) resonator and observe its capacity to trap energy as it is deformed. We define a deformation parameter α, which we will use in the following description as a handle to deform any given geometry, where $\alpha = 0$ indicates the original, undeformed structure and $\alpha > 0$ indicates a proportionally deformed geometry. For example, a circle would be described by $\alpha = 0$, and a deformed circle by $\alpha > 0$, with α describing the degree of deformation. This parameter is generic and can be used to describe the deformation of any type of resonator, for example, square or disk in two dimensions or cube or sphere in three dimensions. In general, the larger α is, the larger the degree of chaos, until a saturation value is reached. The parameter α is defined in equation (1) in the next section.

We begin our analysis with a single *ab initio* numerical experiment, which demonstrates a sixfold increase in the energy stored inside a chaotic resonator with respect to a classical counterpart of the same volume. Such an analytic treatment allows us to study the lifetimes of the electromagnetic modes excited in the cavity and to examine the coherent buildup of energy inside the system. We find that energy is uniformly distributed among the spectral degrees of freedom and that the cavity is able to store the same amount of energy for a given wavelength interval. We support our theoretical results with a set of experiments in both two- and three-dimensional geometries. Two-dimensional resonators were fabricated in planar photonic crystals and analysed by pump-and-probe transmission

[1]PRIMALIGHT, Faculty of Electrical Engineering, Applied Mathematics and Computational Science, King Abdullah University of Science and Technology (KAUST), Thuwal 23955-6900, Saudi Arabia, [2]School of Physics and Astronomy, University of St Andrews, North Haugh, St Andrews KY16 9SS, UK, [3]Department of Astronomy, Bologna University, via Ranzani 1, I-40127, Bologna, Italy, [4]Department of Physics, University of York, Heslington, York YO10 5DD, UK. *e-mail: andrea.fratalocchi@kaust.edu.sa

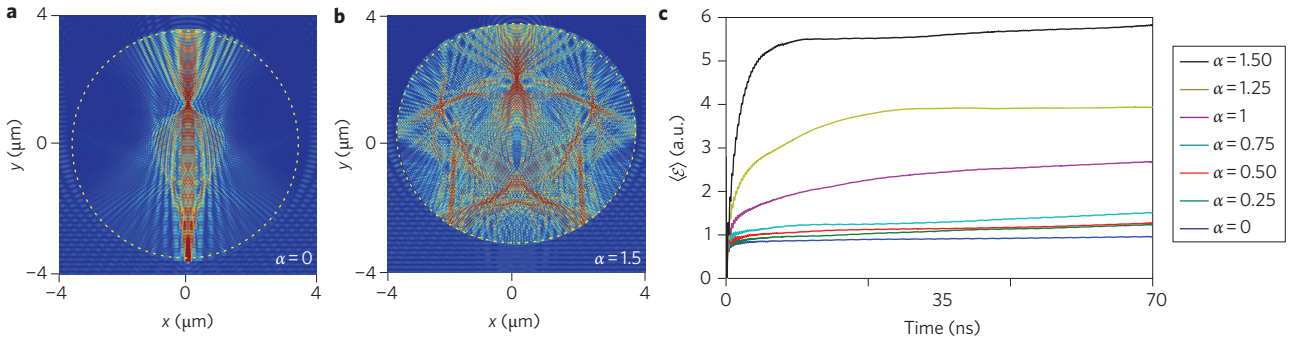

Figure 1 | *Ab initio* results of chaotic energy storage. a, Snapshot of the electromagnetic energy density H distribution after $t = 45$ fs in a resonator (dashed line) with $V = 30\ \mu m^2$ for $\alpha = 0$ (**a**) and $\alpha = 1.5$ (**b**). **c**, Time evolution of the average electromagnetic energy $\langle \mathcal{E} \rangle$ for different α.

measurements. We observed and characterized the resulting modal lifetimes for varying degrees of chaos. While the photonic crystal environment provides fine control over the shape of the resonator, hence its chaotic behaviour, it is difficult to directly measure the energy stored inside the cavity. For this reason, we also studied a three-dimensional arrangement of polystyrene spheres, each suitably modified to exhibit chaotic behaviour. Despite the high transparency of polystyrene, absorption measurements showed a broadband absorption enhancement of ~10% across the entire absorption bandwidth (~450 nm) due to the larger energy trapped in the chaotically deformed resonator. It is worth stressing that the only reason for the increased amount of energy trapped in the resonator is the onset of chaos caused by the deformation of the spheres, with the amount of material being kept strictly constant.

A single *ab initio* experiment

The theory is more easily developed in two dimensions, starting from a circular resonator. Our set-up consists of a silicon dielectric resonator with air holes, the shape of which is defined by the following function in polar coordinates (ρ_c, θ_c):

$$\rho_c = \sqrt{\frac{A}{\pi} - \frac{\alpha^2}{2}} + \alpha \cos\theta_c, \quad 0 \le \theta_c \le 2\pi \tag{1}$$

where A is the resonator area and $\alpha \ge 0$ is the single parameter that controls the resonator shape. Equation (1) belongs to the family of analytic curves investigated by Robnik: for $\alpha > 0$, equation (1) supports chaos in the trajectory of light rays, which randomly bounce inside the resonator[17]. From a physical perspective, the shape defined by equation (1) is equivalent to an asymmetric deformation of a disk, and can be realized experimentally with conventional nanofabrication tools.

In our simulations, we fixed the resonator area to $A = 30\ \mu m^2$ and numerically calculated the electromagnetic energy E stored inside the resonator for varying values of α. Although the value of α in equation (1) is not bound to an upper value, we note that the system reaches saturation for a maximum degree of chaos described by $\alpha = 1.5$ (Supplementary Section SII). We therefore restrict our numerical analysis to $\alpha \in [0,1.5]$. The calculation of the electromagnetic energy $E(t) = \int_{\mathcal{D}} H\ \mathrm{d}\mathbf{r}$ is performed by a numerical integration of the energy density $\mathcal{H}(\rho; t) = 1/2(\mathbf{E} \cdot \mathbf{D} + \mathbf{H} \cdot \mathbf{B})$ in the volume D encompassed by the resonator and defined by $\rho \le \rho_c$ and $0 \le \theta \le 2\pi$. We simulated the input from a supercontinuum source centred at $z = 0$ and propagating along z for wavelengths between $\lambda = 300$ nm and $\lambda = 1{,}300$ nm, which simulates a broadband source such as sunlight. Figure 1a,b shows a time snapshot of the spatial distribution of $\mathcal{H}$ after $t = 45$ fs, and illustrates how the geometry of the resonator changes with α (Fig. 1a,b, dashed line). As seen, even a small deformation in shape (at a constant volume) yields a radically different behaviour in the distribution of light energy inside the resonator. Figure 1c, conversely, displays the time-averaged energy $\langle \mathcal{E} \rangle = 1/t \int_0^t \mathrm{d}t' \mathcal{E}(t')$ evolution with increasing parameter α. Remarkably, the introduction of chaos into the motion of light is accompanied by a dramatic change in the energy stored inside the resonator; indeed, the steady-state regime (when the insertion of energy balances radiation losses) shows an approximately sixfold increase even for $\alpha = 1.5$ (Fig. 1b). This energy accumulation grows with the deformation, and rises monotonically as α increases from 0 to 1.5.

We use time-dependent coupled mode theory (TDCMT)[18] to develop a simple and reliable model for the light–resonator interaction. The system can be modelled as a side-coupled resonator, the dynamical equations of which can be easily solved to obtain energy $\mathcal{E}_k$ and power $\mathcal{P}_k$ stored in the the kth mode (Supplementary Section SI):

$$\mathcal{E}_k = \frac{\tau_k^2}{\tau_e}(1 - e^{-\frac{t}{\tau_k}})^2, \mathcal{P}_k = \frac{2\frac{\tau_e}{\tau_{k0}}}{\left(1 + \frac{\tau_e}{\tau_{k0}}\right)^2}|S|^2 \tag{2}$$

where $|S|$ is the input source power and $(1/\tau_k) = (1/\tau_{k0}) + (1/\tau_e)$ is the mode decay rate ($1/\tau_{k0}$ is the intrinsic cavity decay rate of the kth mode and $1/\tau_e$ is the escape rate due to coupling with the environment). The power $\mathcal{P}_k$ strongly depends on the ratio between the radiation and the coupling loss through the parameter τ_{k0}/τ_e, achieving the maximum value of $\mathcal{P}_k = 0.5|S|^2$ when $\tau_e = \tau_{k0}$. Outside this matching condition, the power coupled into the structure decreases very quickly. To study how the dynamics of the decay rates can be affected by chaos, we began by calculating the evolution of the decay rates τ_{k0} for different α in the resonator defined by equation (1). In a series of finite-difference time-domain (FDTD) simulations, we first excited the resonator with a source and then monitored the energy evolution $\mathcal{E}(t)$ when the source was switched off. The decay constants τ_{k0} are extracted from the time energy evolution $\mathcal{E}(t) = \sum_k |A_k|^2 e^{-2t/\tau_{k0}}$ by applying the Prony method[19]. Figure 2a shows two typical examples of numerical simulations (markers) and a fit (continuous line) for two different values of α. In general, modes of different frequency exhibit different decay rates $1/\tau_{k0}$. However, when strong chaos is generated in the structure, the distribution of τ_{k0} converges towards a frequency-independent delta function. In fact, calculations that start from initial conditions already belonging to the chaotic region of phase space will always be distributed according to the same probability distribution, which defines the so-called 'natural invariant measures' of the system[20]. As a result, when the entire phase space is dominated by chaos, we observe the same

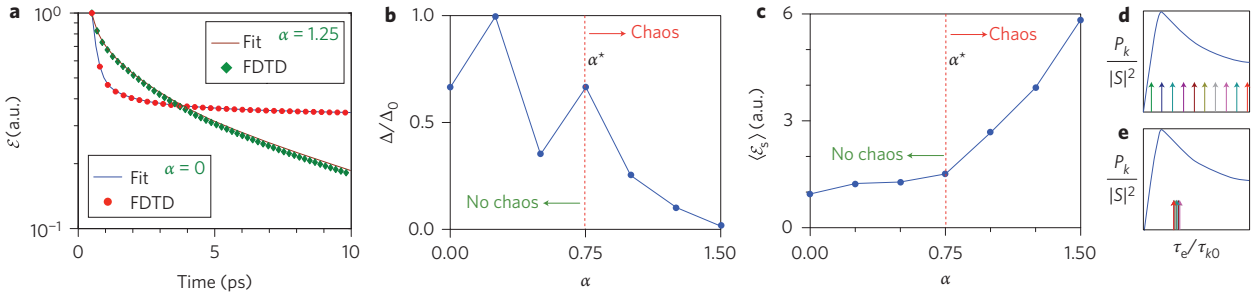

Figure 2 | Chaos-induced modal collapse. a, Log-plot of the energy E relaxation dynamics for $\alpha = 0$ and $\alpha = 1.25$, showing FDTD results (symbols) and Prony exponential fits (solid lines). **b**, Normalized distribution of the difference between the maximum and minimum decay constants $\Delta(\alpha)/\Delta(0) \equiv \Delta/\Delta_0$ versus α. **c**, Steady-state energy distribution $\langle \mathcal{E}_s \rangle = \langle \mathcal{E} \rangle$ ($t = 45$ fs) for varying values of α. **d**,**e**, Effects of convergence of the decay constants τ_k on the power $\mathcal{P}_k$ transferred into the structure. This behaviour is plotted versus τ_e/τ_{k0} as a solid line. In the non-chaotic situation (**d**) the distribution of τ_e/τ_{k0} (coloured arrows) is broad and only a few frequencies efficiently transfer power. In the strongly chaotic case (**e**), conversely, a condensed distribution of τ_e/τ_{k0} yields the same contribution for all wavelengths and a much larger number of frequencies contribute to store energy.

evolution of the decay rates, for all possible initial conditions, towards a frequency-independent decay rate $\tau_{k0} = \tau_0$. A convenient way of highlighting this dynamics is to plot the difference between the maximum and the minimum decay constant, $\Delta(\alpha) = \max(\tau_{k0}) - \min(\tau_{k0})$, for different values of α (Fig. 2b). We clearly observe a transition scenario. Below the chaos threshold, $\alpha \leq \alpha^*$, the dynamics simply shows an oscillation of $\Delta(\alpha)$ around the same average value, while above it ($\alpha \geq \alpha^*$), a clear convergence of $\Delta \to 0$ is observed. The value α^* depends on the specific geometry of the chaotic resonator, and can be assessed by calculating the relative area of the system phase space that encompasses chaos (Supplementary Section SII). The effect of this convergence towards a single lifetime of all the modes on the energy collected by the resonator can be readily evaluated from equation (2). The total power transferred into the structure, in particular, then becomes frequency-independent ($\mathcal{P}_k = \mathcal{P}_0 = 2|S|^2(1 + \tau_e/\tau_0)^{-2}\tau_e/\tau_0$), and every mode contributes to the same extent to storing energy inside the resonator. When many modes are present in the resonator, their large number results in a coherent buildup process that leads to a significant accumulation of energy (Figs 1b, 2c). In the non-chaotic case, conversely, much fewer modes are able to efficiently transfer energy into the resonator due to the mismatch between τ_{k0} and τ_e (Fig. 2d,e) and the system can store relatively less energy (Figs 1b, 2d).

The chaos-assisted energy buildup process observed when $\alpha \geq \alpha^*$ originates from the fundamental thermodynamic principle of equipartition, which can be highlighted using equation (2). By substituting $\tau_{k0} = \tau_0$ into the left-hand side of equation (2), and assuming a dense distribution of modes, with wavelength separation $\lambda_{k+1} - \lambda_k = \mathrm{d}\lambda = \lambda$, we obtain

$$\frac{\partial \mathcal{E}}{\partial \lambda} = \text{const.} = \mathcal{E}_0 \qquad (3)$$

which can be regarded as an equipartition theorem, with the energy equally distributed among all degrees of freedom (that is, the spectral wavelengths) due to the strongly chaotic nature of the system. Equipartition is at the foundation of classical statistical mechanics, and forms the basis for thermodynamic ensembles and the observation of different phases of matter[21]. Applied to photonics, we have the remarkable opportunity of exploiting this principle for enhancing the energy confinement properties of photonic structures. As already discussed above, this opportunity was confirmed by calculating the energy stored for a broadband source in the two limiting conditions of a fully chaotic geometry (Fig. 3, squares) and a non-chaotic geometry (Fig. 3, circles), finding a sixfold enhancement in the chaotic case.

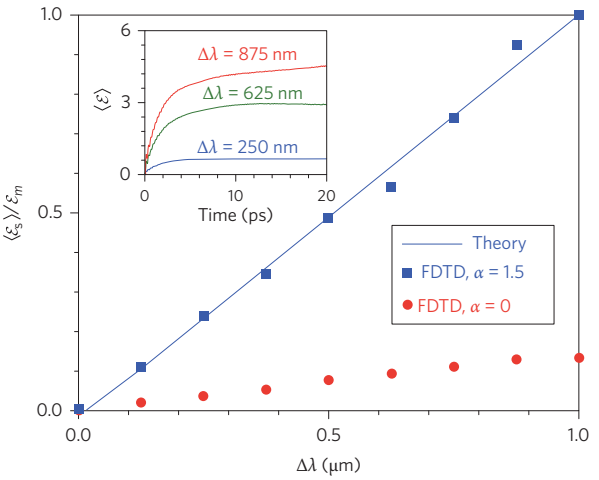

Figure 3 | Results for a variable-bandwidth source. FDTD calculated average energy $\langle \mathcal{E} \rangle$ versus time for $\alpha = 1.5$ and different normalized bandwidth $\Delta\lambda$ symmetrically centred at 800 nm. Inset: FDTD computed steady-state average energy $\langle \mathcal{E}_s \rangle$ versus bandwidth $\Delta\lambda$ for $\alpha = 0$ (circle markers) and $\alpha = 1.5$ (square markers). In **a**, the solid line indicates the behaviour predicted by equation (3). The energy $\langle \mathcal{E}_s \rangle$ is normalized to the maximum value $\mathcal{E}_m$ attained for $\alpha = 1.5$ and $\Delta\lambda = 1\,\mu$m.

Two-dimensional experiments in photonic-crystal cavities

Energy equipartition and chaotic energy harvesting occur because of the convergence of the modal lifetimes towards a single value τ_{k0}. We therefore begin our experiments by investigating the occurrence of this phenomenon in real structures with controllable chaoticity. We designed and experimentally realized a series of planar two-dimensional stadium-shaped resonators in planar photonic crystals fabricated in silicon on insulator (SOI). The substrate consists of a 220-nm-thick silicon layer on a 2-μm-thick insulator buried oxide. The patterns were written into ZEP resist on a modified LEO/RAITH system with 2 nm step size and etched with a 50:50 mixture of SF_6 and CHF_3 gases in a reactive ion etching machine. After stripping the residual resist, the sample was cleaved for end-fire coupling. Figure 4a–c presents a set of scanning electron microscopy (SEM) images that illustrates how the shape of the resonator evolves with a change in the deformation parameter α. The shape starts as a regular square (Fig. 4a) for $\alpha = 0$ and becomes a

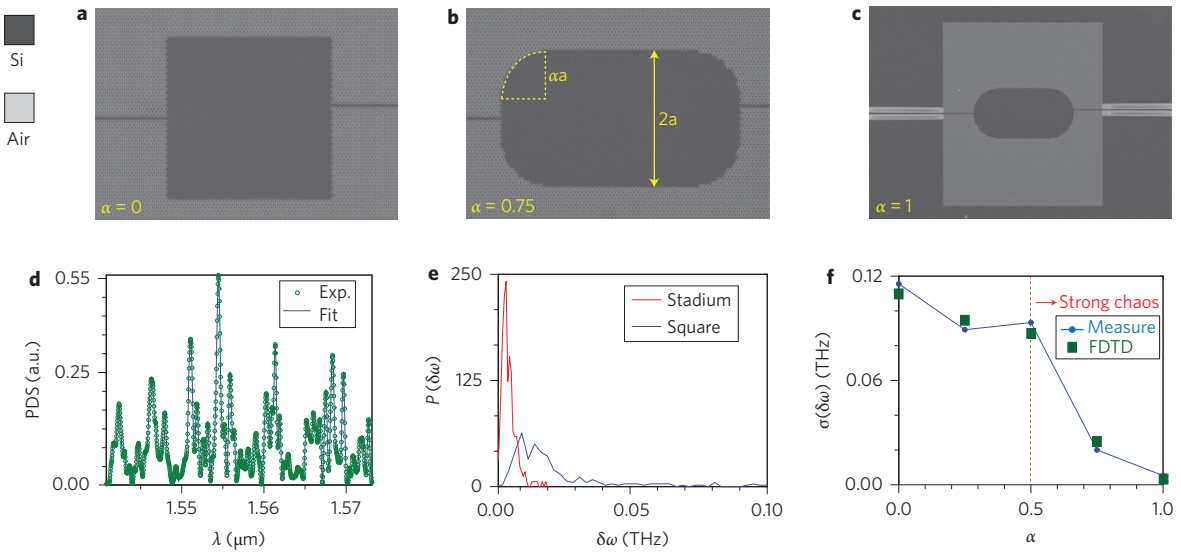

Figure 4 | Summary of two-dimensional experimental results. a–c, SEM images of the sample geometry for $\alpha = 0$ (**a**), $\alpha = 0.75$ (**b**) and $\alpha = 1$ (**c**). **d**, Experimental spectrum (circles) and theoretical reconstruction via wavelet multiscale analysis (solid line) for $A = 400\ \mu m^2$ and $\alpha = 1$; PDS, power density spectrum. **e**, Probability distribution $P(\delta\omega)$ of the resonance widths $\delta\omega$ calculated for the fully chaotic resonator ($\alpha = 1$). **f**, Standard deviation $\sigma(\delta\omega)$ of the resonance widths versus α.

fully chaotic stadium-shaped resonator (Fig. 4c) for $\alpha = 1.5$, with strong chaos already developed for $\alpha > \alpha^* = 0.5$. The parameter $a = \sqrt{A/(4 + \pi\alpha^2)}$ guarantees a constant resonator area A as α is varied (Fig. 4b). As the photonic-crystal lattice was designed to exhibit a bandgap around 1.5 μm with a bandwidth of ~400 nm, any electromagnetic wave in this range is perfectly reflected at the photonic-crystal boundaries, and can only escape via the input/output waveguides of the structure or by scattering at imperfections. The system can therefore be described as a two-dimensional resonator with measurable losses, and the modal decay constants τ_k can be extracted from the transmitted spectrum. We used the multiscale analysis described in ref. 22, which provides an excellent reconstruction technique even when the resonances overlap. The method fits the spectrum by means of a sum of suitable wavelet functions, allowing the wavelength position λ_0 and the width $\delta\lambda$ of each mode to be computed. The resonance widths $\delta\lambda$ are then inversely proportional to the modal decay rates $1/\tau_k = \delta\omega = c\delta\lambda/n\lambda_0^2$ (ref. 18). To collect statistically relevant data, we fabricated several samples with different areas A (400 μm^2, 800 μm^2 and 1,200 μm^2), and for each area we considered five different degrees of chaos, expressed through the deformation parameters $\alpha = 0$, 0.25, 0.5, 0.75 and 1. To characterize the samples, we used polarized light in the wavelength range 1,520–1,620 nm. Figure 4d shows a portion of one of the measured spectra, together with its reconstruction via multiscale analysis[22], which shows a perfect reproduction of the experimental results. All spectra (not shown here) have been reconstructed with the same level of accuracy. We are able to extract ~2,000 resonances for each α, which allows us to extract statistically relevant trends. Figure 4e displays the resonance linewidth probability distribution $P(\delta\omega)$ for $\alpha = 1$ (stadium) and $\alpha = 0$ (square). We note that for $\alpha = 1$, the resonances are strongly converging towards a value of $\delta\omega \approx 5 \times 10^{-3}$ THz with only negligible contributions arising from the short-lived modes that are characterized by a larger $\delta\lambda$. Conversely, in the non-chaotic regime, we observed the presence of many short-lived resonances, indicated by the presence of data points up to, and even beyond 0.1 THz, as well as the wider probability distribution observed at low frequencies. To study the convergence of the lifetimes towards a single value, we group the data for different A and the same α together, and calculate the standard deviation $\sigma(\delta\omega)$ of the resonance widths $\delta\omega$. Figure 4f illustrates the results of this analysis. In perfect agreement with our theoretical predictions and *ab initio* simulations (Fig. 4f, FDTD symbols), we observed a significant narrowing of the linewidth distribution above the threshold for chaos. It is worth highlighting that this convergence of the linewidth towards a single value does not depend on A, but only on α, which is a clear experimental demonstration that the phenomenon relies entirely on the chaotic properties of the motion of light. The consequences of such an experimentally demonstrated collapse are shown in Fig. 5, where we have calculated, by *ab initio* simulations, the energy trapped in the structure. As seen, the energy increases by a factor of 207% in the chaotic structure. Considering the small bandwidth of the signal (~100 nm), this is a remarkable result.

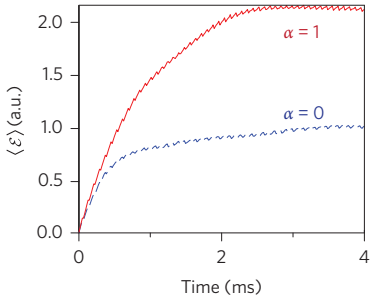

Figure 5 | Energy trapping in two-dimensional resonators. FDTD calculated averaged energy $\langle\mathcal{E}\rangle$ evolution in the two-dimensional photonic-crystal structure in fully chaotic ($\alpha = 1$) and non-chaotic ($\alpha = 0$) conditions.

Three-dimensional experiments with deformed microspheres

An ubiquitous technology should not rely on complicated optimization processes, but should instead be reliable and simple to develop. In the previous section, we tuned the chaoticity of the structure to reach full chaos, thus obtaining a 207% increase in energy. However, even when chaos is not fully developed in phase space, the presence of chaos increases the similarity of the lifetimes and leads to broadband energy storage (Figs 1c, 2b,c). We can therefore exploit chaotic harvesting even for very simple conditions, where

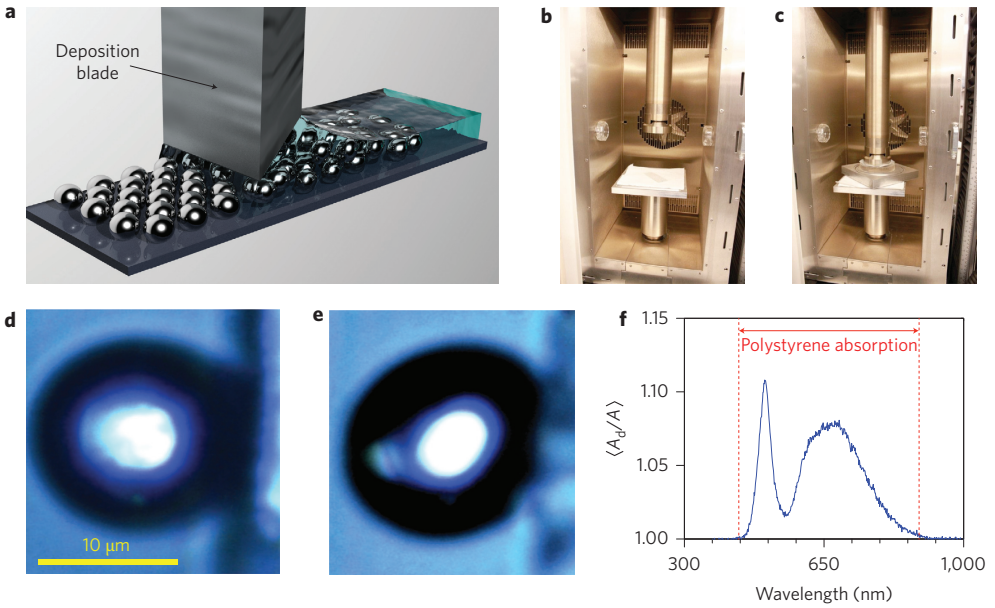

Figure 6 | Summary of the three-dimensional experimental results with deformed microspheres. a, Sketch of monolayer sample fabrication by convective self-assembly. **b**,**c**, Furnace for sample heating and deformation with mechanical pressure. **d**,**e**, SEM images of a microsphere in the original (**d**) and deformed (**e**) case. **f**, Average normalized absorption of the deformed microsphere $\langle A_d \rangle = \langle A_d/A \rangle$, measured for different wavelengths and normalized with respect to the undeformed case A.

fine-tuning of chaos is not provided. We accomplished this final step in a three-dimensional system, which incidentally also proves how the physics of chaotic resonators is independent of the dimensionality of the problem. In particular, we used polystyrene microspheres and studied the absorption when their spherical shape is deformed and the symmetry of the system is broken, thus providing chaotic light motion. Our sample consists of a low-density monolayer of microspheres (Fig. 6a) that are being deformed by mechanical compression (Fig. 6b) in order to obtain an asymmetric shape such as that shown in Fig. 1b. Monolayer fabrication was performed using convective assembly[23,24], where the microspheres are self-assembled on a substrate using a deposition blade (Fig. 6a). The blade height was set at 12 μm from the substrate (sphere size of ∼10 μm) to ensure the formation of a single layer. Following deposition, a glass slide was placed on top of the microspheres for heating and applying mechanical pressure. Deformation was realized by heating the system slightly beyond the glass transition temperature T_g of polystyrene ($T_g = 94\ ^\circ$C; ref. 25), which softens the microspheres sufficiently to deform their shape (Fig. 6b,c). Compression and heating were performed with an Instron 5960 dual column tabletop universal testing system. The pressure force was ramped to 500 N over 2.5 min. Figure 6d,e presents optical micrographs of a microsphere before (Fig. 6d) and after (Fig. 6e) compression, highlighting the asymmetric deformation.

We evaluated the energy harvesting capacity of this system by performing absorption measurements on a single sphere in both deformed and undeformed conditions. To acquire sufficiently large statistics from different input conditions, we placed our sample on a goniometric stage and, through a series of pump-and-probe measurements, calculated the absorption of the sphere at various illumination angles in the range of $\pm 30^\circ$. During each measurement, we illuminated the sphere with a broadband source (consisting of a halogen lamp with bandwidth of ∼1 μm centred at 700 nm) and measured the absorption A from the relation $A = 1 - T - R$, where T and R are the transmittance and reflectance of the microsphere, respectively. To properly collect the scattered light, transmission and reflection spectra were measured in the near field with a lens with a high numerical aperture. The data were acquired with an Ocean Optics QE65000-FL spectrometer. Figure 6f shows the average absorption $\langle A_d \rangle = \langle A_d/A \rangle$ of the deformed system, where A_d and A are the absorption measured in the deformed and undeformed case, respectively. For every angle we obtained an increased absorption due to deformation, with a variance of less than one percent (<0.2%). This originates from the larger electromagnetic energy stored by the microsphere in the deformed case, which led to a higher absorption in the entire absorption window of polystyrene (Fig. 6f). Near the wavelength $\lambda = 450$ nm, in particular, the average absorption increases by ∼12%, whereas in the region where the optical spectrum contains the maximum power (∼600 nm), the absorption shows a broadband increase of ∼6–8%. The chaotic enhancement of the absorption is greater in the spectral region where A is larger and the energy trapped is higher. Outside the absorption frequency window of polystyrene (Fig. 6f, dashed lines), as expected, the chaotic energy accumulation does not induce any measurable variation of the absorption. It is worth noting that an absorption increase of ∼12% over a large bandwidth of 400 nm in a transparent material such as polystyrene is quite a remarkable result.

Discussion

Our results have addressed the problem of light trapping in chaotically deformed resonators and demonstrate the possibility of exploiting equipartition and chaos as a new avenue for energy harvesting. Equipartition, in our case, is manifested by the uniform distribution of energy among all degrees of freedom of the chaotic resonator, that is, the cavity modes. The process is equivalent to the Brownian motion of particles in a liquid, where each particle carries the same amount of energy. In a liquid, the particles always achieve a uniform distribution regardless of the shape of the vessel in which they are contained. In our optical analogue, the steady state of chaotic modes also does not depend on the particular realization of the resonator, but only on its 'macroscopic' geometry, for which the only requirement is to support chaotic trajectories for the trapped light. Besides the obvious implications at the fundamental level, where we demonstrated the existence of a fundamental principle of thermodynamics in the framework of

photonics, our results also have real-world practical implications. The cost of many semiconductor devices, for example, light-emitting diodes and solar cells, is determined to a significant extent by the cost of the material. We show that the functionality of a given geometry can be enhanced up to sixfold by changing the shape alone, that is, without increasing the amount of material and without increasing the material costs. Furthermore, a chaotic system is easier to fabricate as the tolerances are relaxed. Our results can also be extended beyond microresonators, as the phenomenon of chaotic scattering is ubiquitous and also occurs at the nanoscale, that is, when light diffuses into random aggregates of scatterers[26]. We therefore envisage that our ideas will stimulate new research in the assembly of new random nanostructures for efficient energy harvesting.

Methods

***Ab initio* computations.** Numerical simulations were performed with our NANOCPP Maxwell solver (www.primalight.org). NANOCPP is a two/three-dimensional FDTD Maxwell code based on a parallel implementation of the Yee FDTD algorithm. The code makes use of uniaxial perfectly matched layers (UPMLs) to efficiently absorb outgoing waves and provides both hard and planewave sources (the latter via a total field scattered field (TFSF) formulation). NANOCPP efficiently scales over hundreds of thousands of processors, and is specifically designed for massively parallel electromagnetic computations. Our simulations consisted of a parallel study of 40 million single-c.p.u. computational hours, with each simulation employing 8,192 computational cores on the KAUST Shaheen computational cluster and a resolution of 40 points per internal wavelength.

Received 10 September 2012; accepted 15 March 2013; published online 5 May 2013

References

1. Mabuchi, H. & Doherty, A. C. Cavity quantum electrodynamics: coherence in context. *Science* **298,** 1372–1377 (2002).
2. Bourzac, K. Photonic chips made easier. *Nature* **483,** 388 (2012).
3. Kengo, N. *et al.* Ultralow-power all-optical RAM based on nanocavities. *Nature* **6,** 248–252 (2012).
4. Leo, F. *et al.* Temporal cavity solitons in one-dimensional Kerr media as bits in an all-optical buffer. *Nature Photon.* **4,** 471–476 (2010).
5. Atwater, H. A. & Polman, A. Plasmonics for improved photovoltaic devices. *Nature Mater.* **9,** 205–213 (2010).
6. Chalcraft, A. R. A. *et al.* Mode structure of the L3 photonic crystal cavity. *Appl. Phys. Lett.* **90,** 241117 (2007).
7. Campillo, A. J. (ed.) *Optical Processes in Microcavities* (World Scientific, 1995).
8. Gensty, T. *et al.* Wave chaos in real-world vertical-cavity surface-emitting lasers. *Phys. Rev. Lett.* **94,** 233901 (2005).
9. Nöckel, J. U. & Stone, A. D. Ray and wave chaos in asymmetric resonant optical cavities. *Nature* **385,** 45–47 (1997).
10. Harayama, T., Davis, P. & Ikeda, K. S. Stable oscillations of a spatially chaotic wave function in a microstadium laser. *Phys. Rev. Lett.* **90,** 063901 (2003).
11. Gmachl, C. *et al.* High-power directional emission from microlasers with chaotic resonators. *Science* **280,** 1556–1564 (1998).
12. Michel, C., Doya, V., Legrand, O. & Mortessagne, F. Selective amplification of scars in a chaotic optical fiber. *Phys. Rev. Lett.* **99,** 224101 (2007).
13. Lee, T-D. *et al.* Surface-structure-assisted chaotic mode lasing in vertical cavity surface emitting lasers. *Phys. Rev. Lett.* **101,** 084101 (2008).
14. Chen, C. C. *et al.* Transient dynamics of coherent waves released from quantum billiards and analogous observation from free-space propagation of laser modes. *Phys. Rev. Lett.* **102,** 044101 (2009).
15. Brouwer, P. W., Frahm, K. M. & Beenakker, C. W. J. Quantum mechanical time-delay matrix in chaotic scattering. *Phys. Rev. Lett.* **78,** 4737–4740 (1997).
16. Murugan, G. S., Wilkinson, J. S. & Zervas, M. N. Optical microdiscus resonators by flattening microspheres. *Appl. Phys. Lett.* **101,** 071106 (2012).
17. Robnik, M. Classical dynamics of a family of billiards with analytic boundaries. *J. Phys. A* **16,** 3971–3986 (1983).
18. Haus, H. A. *Waves and Fields in Optoelectronics* (Prentice-Hall, 1984).
19. Tijhuis, A. G. *Electromagnetic Inverse Profiling* (VNU Science Press, 1987).
20. Beck, C. & Schlögl, F. *Thermodynamics of Chaotic Systems* (Cambridge Univ. Press, 1993).
21. Gallavotti, G. *Statistical Mechanics: A Short Treatise* (Springer, 1999).
22. Di Falco, A., Krauss, T. F. & Fratalocchi, A. Lifetime statistics of quantum chaos studied by a multiscale analysis. *Appl. Phys. Lett.* **100,** 184101 (2012).
23. Malaquin, L., Kraus, T., Schmid, H., Delamarche, E. & Wolf, H. Controlled particle placement through convective and capillary assembly. *Langmuir* **23,** 11513–11521 (2007).
24. Li, X-H. *et al.* Light extraction efficiency and radiation patterns of III-nitride light-emitting diodes with colloidal microlens arrays with various aspect ratios. *IEEE Photon. J.* **3,** 489–499 (2011).
25. Suh, K. Y., Yoon, H., Lee, H. H., Khademhosseini, A. & Langer, R. Solventless ordering of colloidal particles through application of patterned elastomeric stamps under pressure. *Appl. Phys. Lett.* **85,** 2643–2645 (2004).
26. Ott, E. *Chaos in Dynamical Systems* (Cambridge Univ. Press, 1997).

Acknowledgements

The resources of the Supercomputing Laboratory at King Abdullah University of Science & Technology (KAUST) were used for computer time. A.F. acknowledges funding from KAUST (award no. CRG-1-2012-FRA-005). A.D.F. is supported by an EPSRC Career Acceleration Fellowship (EP/ I004602/1).

Author contributions

A.F. initiated the work and developed the theory behind chaotic energy harvesting. C.L., D.M. and A.F. carried out numerical FDTD simulations and performed data analysis. A.D.F. and T.F.K. realized the photonic-crystal samples and performed the experiments on the two-dimensional geometries. B.S.O., Y.K. and A.F. performed experiments on three-dimensional deformed microspheres. All authors contributed to manuscript preparation.

Additional information

Supplementary information is available in the online version of the paper. Reprints and permissions information is available online at www.nature.com/reprints. Correspondence and requests for materials should be addressed to A.F.

Competing financial interests

The authors declare no competing financial interests.

nature photonics

SUPPLEMENTARY INFORMATION

DOI: 10.1038/NPHOTON.2013.108

Supplementary information: Enhanced energy storage in chaotic optical resonators

C. Liu[1], A. Di Falco[2], D. Molinari[1,3], Y. Khan[1], B. S. Ooi[1], T. F. Krauss[2,4] and A. Fratalocchi[1*]

[1] *PRIMALIGHT, Faculty of Electrical Engineering; Applied Mathematics and Computational Science, King Abdullah University of Science and Technology (KAUST), Thuwal 23955-6900, Saudi Arabia*

[2] *School of Physics and Astronomy, University of St. Andrews, North Haugh, St. Andrews KY16 9SS, UK*

[3] *Dept. of Astronomy, Bologna University, via Ranzani 1, I-40127, Bologna, Italy.*

[4] *Dept. of Physics, University of York, Heslington, York, YO10 5DD, UK*

(Dated: March 9, 2013)

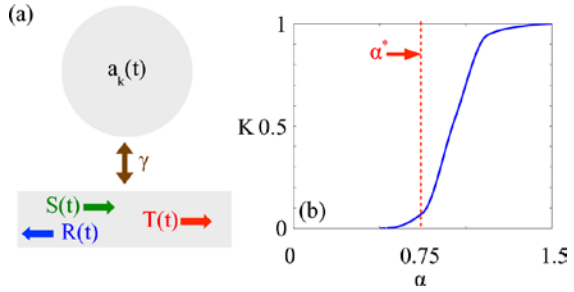

FIG. 1. Coupled mode theory modelling and characterisation of chaos. (a) light-cavity interaction TDCMT scheme: $S(t)$ is the input source, $R(t)$, $T(t)$ are reflection and transmission signals, respectively, a_k is the k-th mode in the resonator and γ is the coupling coefficient between the resonator and the external environment; (b) normalised entropy K versus chaotic degree α for the Robnik billiard expressed by Eq. (1) of the main text.

I. TIME DEPENDENT COUPLED MODE EQUATIONS

Figure 1a shows a TDCMT model of the light-resonator system. In this scheme, the environment is represented as a waveguide side coupled to the resonator. The input signal $S(t)$ interacts with the resonator through the coupling coefficient γ and transfers energy to the modes of the cavity $a_k(t) = A_k e^{i\omega_k t - t/\tau_k}$ ($k \in [1, N]$), being ω_k the frequency, $\frac{1}{\tau_k}$ the lifetime, A_k the amplitude and $\mathcal{E}_k = |a_k|^2$ the energy carried by the $k-$th mode. The total energy stored in the resonator is $\mathcal{E} = \sum_k \mathcal{E}_k$. Decay rates $\frac{1}{\tau_k}$ can be further decomposed as follows $\frac{1}{\tau_k} = \frac{1}{\tau_{k0}} + \frac{1}{\tau_e}$, with $\frac{1}{\tau_{k0}}$ the intrinsic decay constant of the mode and $\frac{1}{\tau_e}$ the decay constant due to coupling with the source. Cavity modes obey the following evolution equations [1]:

$$\frac{da_k}{dt} = \left[i\omega_k - \left(\frac{1}{\tau_k}\right)\right] a_k + \gamma \cdot S(t), \quad k \in [1, ..., n], \quad (1)$$

with $\gamma = \sqrt{\frac{1}{\tau_e}}$ [1], while reflection $R = \sum_k R_k$ and transmission $T = \sum_k T_k$ are given by the following expressions:

$$R_k = -\sqrt{\frac{1}{\tau_e}} a_k, \qquad T_k = -\sqrt{\frac{1}{\tau_e}} + S, \quad (2)$$

with R_k and T_k the reflection and transmission of the $k-$th mode, respectively [1]. In the presence of a single frequency excitation $S = e^{i\omega t}\Theta(t)$ switched on at $t = 0$, with $\Theta(t)$ being the Heaviside function, Eqs. (1) are readily solved for each a_k and read:

$$a_k = \sqrt{\frac{1}{\tau_e}} \frac{e^{i\omega t} - e^{i\omega_k t - t/\tau_k}}{i(\omega - \omega_k) + \frac{1}{\tau_k}}. \quad (3)$$

For a broadband source, $S = \int d\omega e^{i\omega t}\Theta(t)$, the total electromagnetic energy $\mathcal{E} = \sum_k |a_k|^2$ stored in the cavity is readily found to be:

$$\mathcal{H} = \int \frac{d\omega}{\tau_e} \sum_k \frac{1 + e^{-\frac{2t}{\tau_k}} - 2\cos[(\omega_k - \omega)t] e^{-\frac{t}{\tau_k}}}{(\omega_k - \omega)^2 + \frac{1}{\tau_k^2}}. \quad (4)$$

Equation (4) can be further simplified as the integral yields significant contributions only for $\omega \approx \omega_k$, and we obtain:

$$\mathcal{H}\tau_e \approx \sum_k \tau_k^2 \left(1 - e^{-\frac{t}{\tau_k}}\right)^2, \quad (5)$$

The power $\mathcal{P}_k$ transferred into the $k-$th mode is conversely evaluated from the energy balance equation:

$$\frac{\partial |a_k|^2}{\partial t} = \mathcal{P}_k = |S|^2 - |R_k|^2 - |T_k|^2, \quad (6)$$

that, in conjunction with Eqs. (2)-(3), yields:

$$\mathcal{P}_k = \frac{2\frac{\tau_e}{\tau_{k0}}}{\left(1 + \frac{\tau_e}{\tau_{k0}}\right)^2} |S|^2, \quad (7)$$

II. CHARACTERISATION OF CHAOS

We quantitatively describe the chaoticity of light motion by evaluating the relative area of the resonators phase space that encompasses chaos. This is achieved by first calculating the distribution of the Lyapunov exponent [2] in phase space, and then performing a weighted summation by assigning '1' if the Lyapunov exponent is

* andrea.fratalocchi@kaust.edu.sa; www.primalight.org

DOI: 10.1038/NPHOTON.2013.108

positive, and '0' otherwise. The resulting quantity K can be regarded as a normalised version of the Kolmogorov-Sinai entropy [2, 3]. In particular, when $K = 0$, the resonator dynamics exhibits no chaos and the resulting motion is totally reversible, while for $K = 1$ the phase space is totally chaotic and all input conditions lead to chaos. Values of K between these two limiting conditions indicate a phase space partially chaotic, with K measuring the relative area of the chaotic sea with respect to the reversible portion of the dynamics. Figure 1b displays the behaviour of K for the billiard expressed by Eq. (1) of the main text (Robnik curve). For α lower than the threshold value $\alpha^* = 0.75$, no chaos is observed in the structure, while for $\alpha > \alpha^*$ strong chaos is generated through the shape deformation. At $\alpha = 1.5$, the structure is fully chaotic and the phase-space is totally dominated by a single chaotic sea.

[1] Haus, H. A. *Waves and Fields in Optoelectronics* (Prentice-Hall, Englewood Cliffs, N. J., 1984).
[2] Ott, E. *Chaos in Dynamical Systems* (Cambridge University Press, Cambridge, 1997).
[3] Boffetta, G., Cencini, M., Falcioni, M. & Vulpiani, A. Predictability: a way to characterize complexity. *Physics Reports* **356**, 367 – 474 (2002).